

Analyzing the measured phase in the multichannel Aharonov-Bohm interferometer

M. Țolea¹, M. Niță¹, A. Aldea^{1,2}

¹ *National Institute of Materials Physics, POB MG-7, 77125 Bucharest-Magurele, Romania.*

² *Institute of Theoretical Physics, Cologne University, 50937 Cologne, Germany.*

We address the quantum dot phase measurement problem in an open Aharonov-Bohm interferometer, assuming multiple transport channels. In such a case, the quantum dot is characterized by more than one intrinsic phase for the electrons transmission. It is shown that the phase which would be extracted by the usual experimental method (i.e. by monitoring the shift of the Aharonov-Bohm oscillations, as in Schuster *et al.*, Nature **385**, 417 (1997)) does not coincide with any of the dot intrinsic phases, but is a combination of them. The formula of the measured phase is given. The particular case of a quantum dot containing a $S = 1/2$ spin is discussed and variations of the measured phase with less than π are found, as a consequence of the multichannel transport.

I. INTRODUCTION

The recent developments in the building of mesoscopic devices allow to measure the phase (phase shift) of the electronic wave function after it is scattered by a quantum dot. Yacoby *et al.* [1], placed a quantum dot in one of the arms of a quantum ring, realizing an Aharonov-Bohm (AB) interferometer and performed for the first time a phase measurement. In order to avoid multiple encirclements of the ring, Schuster *et al.* [2] went a step further and opened the Aharonov-Bohm interferometer by adding a number of additional leads (see also [4, 5] and [6, 7] about the conditions of opening the interferometer). In this case, the electronic waves that reach the drain, have passed through the dot and through the reference arm only once, with the amplitudes $t_{dot} = |t_{dot}|e^{i\phi_{dot}}$ and $t_{ref} = |t_{ref}|e^{i\phi_{ref}}$ respectively, yielding the total transmittance through the interferometer:

$$T_{int} = |t_{dot}|^2 + |t_{ref}|^2 + 2|t_{dot}||t_{ref}|\cos(\phi_{dot} - \phi_{ref}). \quad (1)$$

The dot phase ϕ_{dot} is extracted from Eq.1 by varying the magnetic flux through the interferometer, and in [2] a phase lapse of π was found, between any pair of consecutive resonances. The expected behavior would have been a phase increase by π on each resonance (which concordates with the experimental findings), but also a constant value of the phase between resonances (when the dot occupancy does not change), as suggested by the Friedel sum rule [3]. The universal phase lapse behavior found by [2] is one of the longest-standing puzzles in mesoscopic physics, which lead to numerous theoretical studies -e.g. [4, 8–10]- the issue being still under debate.

In 2005, Avinun-Kalish *et al.* [11] launched a couple of new puzzles when performing phase measurements on a quantum dot that was initially empty and then gradually filled with electrons. Their experiment showed that the phase lapse of π was actually not universal, as found in [2], but appears after the dot is occupied with several electrons. In the few-electrons regime, the phase variation shows a different behavior, also intriguing: one could notice a number of dips in the phase evolution of amplitude less than π , attributed by the authors to the Kondo effect. However, other experimental papers that addressed the phase measurement in the Kondo regime (e.g. [12]) reported a different behavior, namely an increase of the phase by $\pi/2$ on the resonance, which then remains constant at this value. The paper of Avinun-Kalish *et al.* [11] opened a new trend of calculations on few-electrons systems (e.g. [13–18]). The reduced variation of the phase on and between (some) resonances, in the few-electrons regime, is a new puzzle in mesoscopic physics, and one of the motivations of our paper. We will show that the existence of multiple transport channels can lead to a reduced variation of the measured phase.

To illustrate our statement, we shall address the scattering of an electron through a quantum dot with a $S = 1/2$ magnetic impurity. The model has the advantage of being exactly solvable, while being a good approximation for the case when one electron is located in the dot, and another -itinerant- electron is scattered. Some authors proposed more complex models for impurity dots, e.g. [19–23], but this is not a purpose of this paper, where a simple model is needed to set the focus on the phase measurement procedure.

The scattering of an electron on an impurity that possesses internal degrees of freedom was addressed before in mesoscopic physics, e.g by Mello *et al.* [24], but not in the context of the interferometry and phase measurement.

The outline of the paper is as follows: in section II we describe the transport through the multichannel interferometer and derive the formula of the measured phase; sections III and IV address the case of a quantum dot with a magnetic impurity; the conclusions are given in section V.

II. THE MEASURED PHASE

We consider an open Aharonov-Bohm interferometer, sketched in Fig.1. The term "open" is used in the sense of [2, 4–7], meaning that multiple encirclements of the ring are neglected and only one interference is assumed between the partial electronic waves traveling through the upper and lower arms, respectively. The upper arm has an embedded quantum dot and the lower arm is the reference arm. The two arms enclose a magnetic flux Φ . The interferometer is connected to two transport leads, left (L) and right (R).

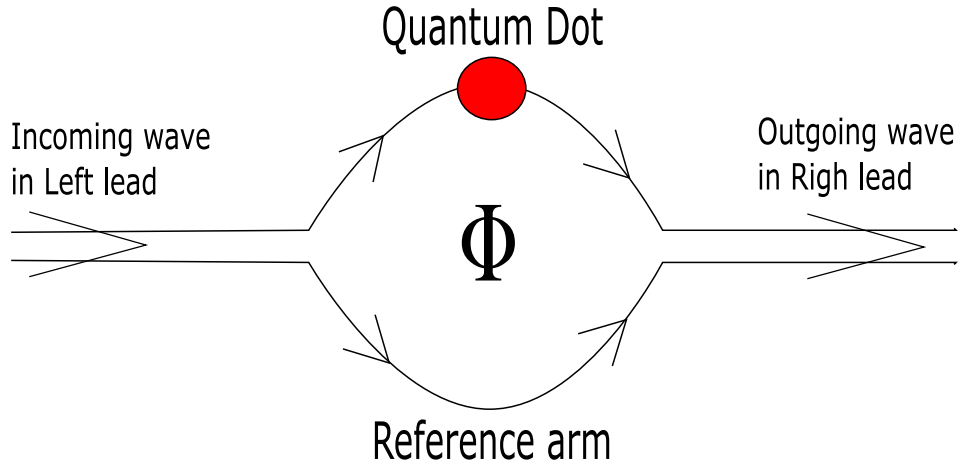


FIG. 1: (Color online) Scheme of the Aharonov-Bohm interferometer.

We consider multiple electron transport channels, denoted with m . For every pair of incoming and outgoing channels (m, m'), there is a tunneling process through the dot that has a tunneling amplitude $t_{m',m}$. The phases $\phi_{m',m} = \text{Arg}(t_{m',m})$ are called intrinsic dot phases. For the tunneling amplitude through the reference arm, $t_{ref} = |t_{ref}|e^{i\phi_{ref}}$, the phase can be set equal to the magnetic flux through the ring $\phi_{ref} = \Phi$ (and in the numerical calculations we will take $|t_{ref}| = 1$).

We are interested in calculating the total transmittance through the open interferometer, which is the experimentally available quantity. Incoherent leads are considered, for which the incident electron comes through each of the channels $m = 1, \dots, M$ with equal probability $1/M$. After a straightforward calculation (see Appendix A), the total transmittance through the interferometer can be expressed:

$$T_{int} = T_{dot} + |t_{ref}|^2 + \frac{2}{M}|t_{ref}| \sum_m |t_{m,m}| \cos(\phi_{m,m} - \Phi), \quad (2)$$

with $T_{dot} = 1/M \sum_{m,m'} |t_{m,m'}|^2$. Now we define the quantity t_{phase} :

$$t_{phase} \equiv \frac{1}{M} \sum_m t_{m,m}, \quad (3)$$

and its phase $\phi_{exp} = \text{Arg}(t_{phase})$. With these notations, the total transmittance reads:

$$T_{int} = T_{dot} + |t_{ref}|^2 + 2|t_{ref}||t_{phase}| \cos(\phi_{exp} - \Phi). \quad (4)$$

The above formula resembles Eq.1, but it is no longer the simple interference of just two waves. In the experiments [2, 11, 12], the transmittance through the interferometer exhibits AB oscillations when Φ is varied and from the shift of the oscillations (when a gate is applied on the dot, for instance) one extracts the evolution of the measured phase. From Eq.4, it is clear that the measured phase is, in the multichannel case, ϕ_{exp} which can be expressed:

$$\cos \phi_{exp} = \frac{\sum_m |t_{m,m}| \cos \phi_{m,m}}{\sqrt{(\sum_m |t_{m,m}| \cos \phi_{m,m})^2 + (\sum_m |t_{m,m}| \sin \phi_{m,m})^2}}. \quad (5)$$

The above formula is the main formal result of the paper. When the transport is single-channel, it is obvious that the measured phase ϕ_{exp} is equal to the intrinsic dot phase; for the multichannel transport, the above formula gives the value of the measured phase ϕ_{exp} in terms of the dot intrinsic phases $\phi_{m,m}$ and amplitude modules $|t_{m,m}|$.

Eq. 5 already allows us to make a comment regarding the evolution of ϕ_{exp} , if we assume that $t_{m,m}$ are of resonance type, with the module presenting a maxima at the resonant energy and the phase increasing, for instance, from 0 to π on the resonance width. Then between consecutive (in-phase) resonances, one has to add two complex numbers that are out of phase. This leads to a smaller amplitude of t_{phase} , but also to a reduced variation of its phase, in the regions where the resonances overlap. We will show this explicitly in the example presented in the following.

III. QUANTUM DOT WITH A MAGNETIC IMPURITY

In this section and the next one, we will describe in detail an example of multichannel scattering, with the aim to obtain in the end the formula of the measurable phase (with the standard experimental method [2, 11, 12]), for the example considered.

We consider here a quantum dot containing a $S = 1/2$ magnetic impurity, which interacts with the itinerant electrons via an exchange interaction. First, one must define the scattering channels and calculate the tunneling amplitudes. According to the standard scattering theory, the impurity dot represents a target that possesses internal degrees of freedom (the impurity may flip its spin) and, in such a case, the scattering channels ($|m\rangle$) are the states of the electron+impurity system: $|\uparrow\uparrow\rangle, |\downarrow\downarrow\rangle, |\uparrow\downarrow\rangle$, and $|\downarrow\uparrow\rangle$, where the simple arrow stands for the spin of the itinerant electron and the double arrow stands for the spin of the impurity (see also [25], where the same basis is used to study the spin transmittance through a closed interferometer).

The Hamiltonian of the dot corresponds to the spin interaction between the electron and impurity:

$$H^D = -J\vec{s}\vec{S} = -J(s_z S_z + \frac{1}{2}s_+ S_- + \frac{1}{2}s_- S_+) \quad (6)$$

The terms in the Hamiltonian can be written in detail:

$$\begin{aligned} s_z S_z &= \frac{1}{4}|\uparrow\uparrow\rangle\langle\uparrow\uparrow| + \frac{1}{4}|\downarrow\downarrow\rangle\langle\downarrow\downarrow| \\ &\quad - \frac{1}{4}|\downarrow\uparrow\rangle\langle\downarrow\uparrow| - \frac{1}{4}|\uparrow\downarrow\rangle\langle\uparrow\downarrow|, \\ s_+ S_- &= |\uparrow\downarrow\rangle\langle\downarrow\uparrow|, \\ s_- S_+ &= |\downarrow\uparrow\rangle\langle\uparrow\downarrow|. \end{aligned} \quad (7)$$

The quantum dot site index (n_D in Appendix B, where the general case is addressed) can be omitted, since the dot is single-site, and there is no risk for confusions (we write for instance $|\uparrow\uparrow\rangle$ for the dot site, instead of $|n_D, \uparrow\uparrow\rangle$).

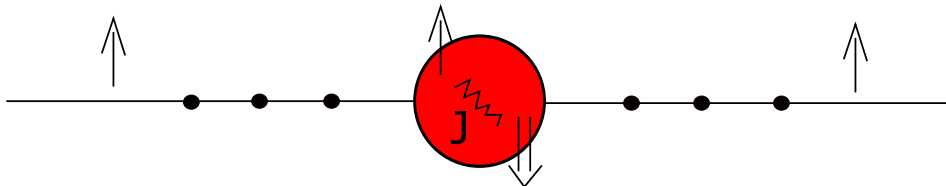


FIG. 2: (Color online) Scheme of the quantum dot containing a magnetic impurity, which interacts with the itinerant electrons through an exchange interaction J . The dot is connected to discrete leads.

To calculate the tunneling amplitudes, we connect the dot to discrete leads, see Fig.2 (for a comparison between discrete and continuous models in mesoscopic physics, see [26]). The hopping constant between the dot and the leads is τ , and the hopping between the leads neighboring sites is τ_l (in the numerical calculations we will take $\tau_l = 1$).

Applying the general recipe in Appendix B (see also [27, 28] for equivalent demonstrations) for the particular case of a single site dot and four transport channels, one writes the effective Hamiltonian (which later shall be used to express the tunneling amplitudes):

$$H_{eff}^D = \begin{bmatrix} -J/4 + x & 0 & 0 & 0 \\ 0 & -J/4 + x & 0 & 0 \\ 0 & 0 & J/4 + x & -J/2 \\ 0 & 0 & -J/2 & J/4 + x \end{bmatrix}, \quad (8)$$

where $x = 2\tau^2 e^{-ik}$ and the columns and rows correspond to the following counting of channel vectors: $|\uparrow\uparrow\rangle, |\downarrow\downarrow\rangle, |\uparrow\downarrow\rangle$ and $|\downarrow\uparrow\rangle$.

Finally, as shown in Appendix B, the tunneling amplitudes between the channels m and m' can be expressed as:

$$t_{m',m} = 2i \frac{\tau^2}{\tau_l} \sin(k) \langle m' | \frac{1}{E - H_{eff}^D} | m \rangle, \quad (9)$$

There are six possible processes, corresponding to the non-zero elements of $1/(E - H_{eff}^D)$, and respecting the total spin conservation. To simplify the index notation, the non-vanishing tunneling amplitudes will be denoted by t_i with $i = 1 \dots 6$:

$$\begin{aligned} 1) & \quad |\uparrow\uparrow\rangle \rightarrow |\uparrow\uparrow\rangle; \quad t_{\uparrow\uparrow,\uparrow\uparrow} = t_1 = |t_1|e^{i\phi_1}, \\ 2) & \quad |\uparrow\downarrow\rangle \rightarrow |\uparrow\downarrow\rangle; \quad t_{\uparrow\downarrow,\uparrow\downarrow} = t_2 = |t_2|e^{i\phi_2}, \\ 3) & \quad |\downarrow\uparrow\rangle \rightarrow |\uparrow\downarrow\rangle; \quad t_{\uparrow\downarrow,\downarrow\uparrow} = t_3 = |t_3|e^{i\phi_3}, \\ 4) & \quad |\downarrow\uparrow\rangle \rightarrow |\downarrow\uparrow\rangle; \quad t_{\downarrow\uparrow,\downarrow\uparrow} = t_4 = |t_4|e^{i\phi_4}, \\ 5) & \quad |\uparrow\downarrow\rangle \rightarrow |\downarrow\uparrow\rangle; \quad t_{\downarrow\uparrow,\uparrow\downarrow} = t_5 = |t_5|e^{i\phi_5}, \\ 6) & \quad |\downarrow\downarrow\rangle \rightarrow |\downarrow\downarrow\rangle; \quad t_{\downarrow\downarrow,\downarrow\downarrow} = t_6 = |t_6|e^{i\phi_6}. \end{aligned} \quad (10)$$

From the spin rotation symmetry of the dot Hamiltonian, one has:

$$\begin{aligned} t_1 &= t_6, \\ t_2 &= t_4, \\ t_3 &= t_5. \end{aligned} \quad (11)$$

During the processes 3 and 5, the spins flip (see [29] for a discussion on the importance of spin-flip processes for open and closed interferometers), while the others are non-flip processes.

In Fig.3 we plot the amplitude modulus and phases for the three tunneling processes t_1 , t_2 and t_3 versus the energy of the incident electron. One notices that t_1 is a single resonance process, while t_2 and t_3 have two resonances each. The single-resonance process, t_1 , has the classical Breit-Wigner structure, and the phase increases by π on the resonance width.

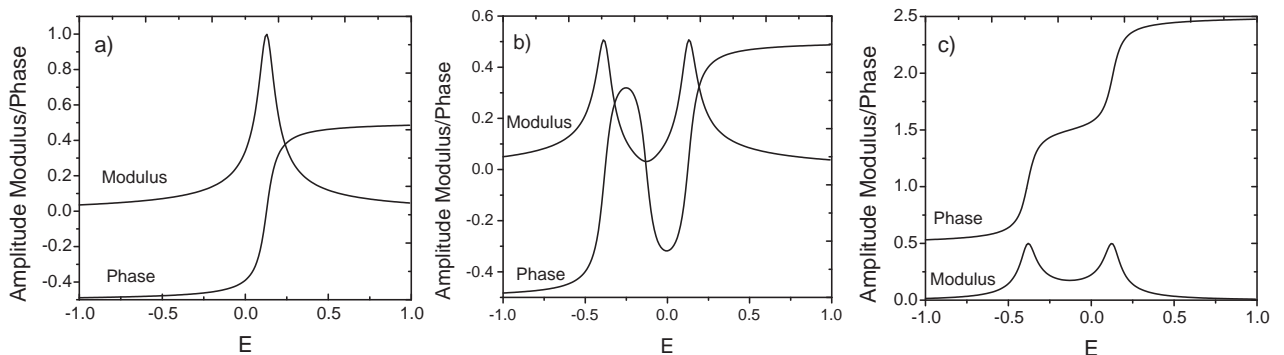


FIG. 3: The modulus and the phase (in π units) of the tunneling amplitude for the three processes a) t_1 , b) t_2 and c) t_3 , plotted versus the energy of the incident electron. The parameters are: $J = -0.5$, $\tau = 0.15$.

The processes with two resonances have different structures and they are of two types: with the two resonances in-phase (t_2) or out-of-phase (t_3). For the in-phase case, plotted in Fig.3b (t_2), the phase increases from $-\pi/2$ to approx 0.3π for the first resonance, then decreases between the resonances to the value -0.3π and finally an increase to $\pi/2$ is noticed on the second resonance. In this case, the tunneling amplitude between resonances is lowered, approaching *zero*. For the out-of phase resonances, Fig.3c (t_3), the phase evolution is different, in the sense that the

phase evolves from $\pi/2$ to $3\pi/2$ for the first resonance, and from $3\pi/2$ to $5\pi/2$ for the second resonance. Between resonances, the phase is roughly constant and the tunneling amplitude is increased.

The above discussed behavior of the tunneling amplitudes can be understood if we perform a spectral decomposition of the dot Hamiltonian. It is straightforward to show that the dot eigenstates are: one singlet state with the energy $E_S = 3J/4$ and three triplet states with $E_T = -J/4$. We define t_S as the tunneling amplitude for the singlet state and t_T the tunneling amplitude for the triplet states. One has $t_S = i\tau^2 \sin(k)(\langle \uparrow\downarrow | - \langle \downarrow\uparrow |)(E - H_{eff}^D)^{-1}(|\uparrow\downarrow\rangle - |\downarrow\uparrow\rangle) = 2i\tau^2 \sin(k)/(E - 3J/4 - 2\tau^2 e^{-ik})$. Similarly, one obtains $t_T = 2i\tau^2 \sin(k)/(E + J/4 - 2\tau^2 e^{-ik})$. The tunneling processes discussed above, $t_{1,2,3}$, can be expressed in the terms of singlet and triplet (this results straightforwardly from the definition Eq.9; see also [30]):

$$\begin{aligned} t_1 &= t_T, \\ t_2 &= \frac{1}{2}(t_T + t_S) \text{ in phase}, \\ t_3 &= \frac{1}{2}(t_T - t_S) \text{ out of phase}. \end{aligned} \tag{12}$$

The sign between the triplet and singlet amplitudes (t_T and t_S) in Eqs.12 explain the in-phase and out-of phase behavior seen in Fig.3b and c.

Now we can calculate the total transmittance of the dot, T_{dot} , by summing for all incoming channels (the probability of finding the incoming electron and the impurity in a given spin configuration is 1/4):

$$T_{dot} = \frac{1}{4} \sum_{i=1}^6 |t_i|^2 = \frac{1}{2} \sum_{i=1}^3 |t_i|^2. \tag{13}$$

Furthermore, by using Eqs.12, the dot transmittance becomes $T_{dot} = 1/4|t_S|^2 + 3/4|t_T|^2$, showing that the singlet resonance is three times lower in amplitude than the triplet resonance (see Fig.4a, where for negative J the singlet resonance is lower in energy), which is an expected result for the two-spin scattering. We mention that this 1/3 ratio in the resonances amplitude was also found by Rejec et. al.[31] for the case of two electrons scattering and the result was used to give a possible explanation of the 0.25 and 0.75 anomalies in quantum wires.

IV. THE MEASURED PHASE OF THE MAGNETIC IMPURITY DOT

Let us now place the impurity dot in one of the arms of an open Aharonov-Bohm interferometer. The total interferometer transmittance is the one given by Eq.4, where $t_{phase} = \frac{1}{4}(t_1 + t_2 + t_4 + t_6) = \frac{1}{2}(t_1 + t_2)$. Using the spectral decomposition (Eqs.12), one can write equivalently:

$$t_{phase} = \frac{1}{4}(3 \cdot t_T + t_S). \tag{14}$$

In Fig.4a we plot the quantum dot transmittance T_{dot} , given by Eq.13, and the measured phase $\phi_{exp} = Arg(t_{phase})$ versus the energy of the incident electron. One can notice that the phase has a reduced variation (by less than π) both on the dot resonances and between them.

The Aharonov-Bohm oscillations of the interferometer transmittance T_{int} are plotted in Fig.4b versus the magnetic flux, in order to reproduce the experimental method [2, 11]. Then, from the horizontal shift of the Aharonov-Bohm oscillations, one extracts the quantum dot "measured" phase evolution, plotted in Fig.4a. The dotted vertical line in Fig.4b is guide for the eye to see the phase evolution. For the lowest curve (corresponding to $E = -0.6$) one reads a phase ϕ_{exp} of about $-\pi/2$ at zero flux (this means that we have neither a maximum of the oscillation, nor a minimum, but a value in the middle). The phase then increases, as the energy of the incoming electron increases, till the oscillations present a maximum at $\Phi = zero$ (see the fifth curve from bottom); this means $\phi_{exp} = 0$ (from Eq.4 one sees that, at $zero$ magnetic flux, $\Phi = 0$, the oscillation presents a maximum if, and only if, $\phi_{exp} = 0$). The phase continues to increase a bit more, and then the AB oscillations begin to shift in the opposite direction, meaning that the phase starts to decrease, and so on, resulting the phase evolution in Fig.4a. For the considered parameters, the measured phase increases with $\sim 0.65\pi$ on the singlet resonance, then decreases with $\sim 0.55\pi$ between resonances, to finally increase again with $\sim 0.9\pi$ on the triplet peak. Even if the shape of the phase evolution does not coincide with the features in [11] - and a more realistic many-body model may be required - the fact that the measured phase evolves with less than π is recovered by our multi-channel model.

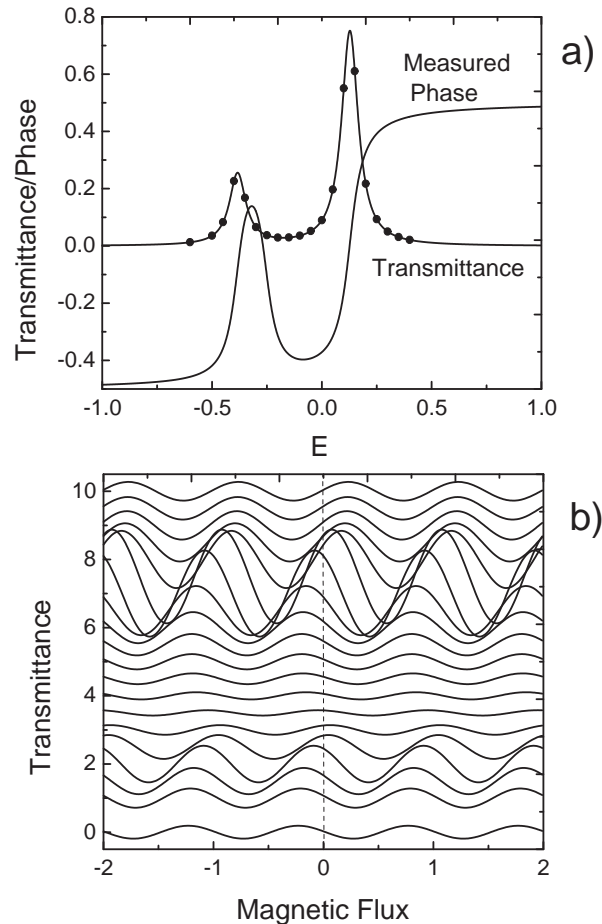


FIG. 4: a) The transmittance through the quantum dot with a $S = 1/2$ magnetic impurity (T_{dot}), and the measured phase (ϕ_{exp} , given in π units), plotted versus the energy of the incident electron; the parameters are: $J = -0.5$, $\tau = 0.15$. b) Total transmittance of the interferometer (T_{int}) versus the magnetic flux (in flux quanta) for the energies $E \in [-0.6, 0.4]$ marked with dots in (a) ($E = -0.6$ corresponds to the lowest curve). The curves are shifted on the vertical for the clarity of presentation. From the horizontal shift of the Aharonov-Bohm oscillations, one can extract the value of the measured phase for different energies.

V. CONCLUSIONS

An experimental method to extract the quantum dot phase, by monitoring the Aharonov-Bohm oscillations of an open interferometer, was developed in previous works (e.g. [2, 11, 12]).

In this paper we show that, when the transport is multichannel, the phase extracted by using the mentioned method is not an intrinsic dot phase. Instead, it is the phase of the sum of the diagonal dot tunneling amplitudes.

We paid a particular attention to the situation when an electron is scattered by a potential that mixes the transport channels. To this purpose, we have analyzed the particular case of a quantum dot containing a $S = 1/2$ magnetic impurity. For this simple model, we have found variations of the measured phase with less than π , both on the resonances and between them. This reproduces some features of a recent experiment [11] and is, in our case, a consequence of the multi-channel transport.

VI. ACKNOWLEDGEMENTS

We acknowledge support from PNCDI II programme under contract No. 515/2009, Contract Nucleu 45N/2009, and of Sonderforschungsbereich 608 at the Institute of Theoretical Physics, University of Cologne.

Appendix A: Total transmittance through a multichannel open interferometer with embedded quantum dot

The measurable quantity in interference experiments is the total transmittance through the interferometer. To express this, we need the scattering solutions of the Schrodinger equation. First, we chose the wave function in the left lead to describe the physical situation when an incident electron is coming from the left lead in a selected channel m and is reflected back with the amplitude $r_{m',m}$ into the channel m' :

$$|\Psi^{L,m}\rangle = \sum_{n \in L} e^{ikn} |n, m\rangle + \sum_{n \in L, m'} e^{-ikn} r_{m',m} |n, m'\rangle. \quad (\text{A1})$$

The wave function in the right lead describes the transmitted electron and for the open interferometer it is considered to be the sum of the two wave functions that correspond to the two paths: reference and QD arms. The tunneling amplitude through the reference arm does not depend on the transport channel m , $t_{ref} = |t_{ref}|e^{i\phi_{ref}}$, and the corresponding wave function is:

$$|\Psi_{ref}^{R,m}\rangle = t_{ref} \sum_{n \in R} e^{-ikn} |n, m\rangle. \quad (\text{A2})$$

On the contrary, the tunneling amplitudes for the electron that passes the quantum dot arm depend on the incoming and outgoing transport channels m and m' , and the wave function reads:

$$|\Psi_{QD}^{R,m}\rangle = \sum_{n \in R, m'} t_{m',m} e^{-ikn} |n, m'\rangle, \quad (\text{A3})$$

where $t_{m',m}$ is the transmission amplitude of the quantum dot for an electron coming in channel m and transmitted in channel m' .

The interference wave function in the right lead of the AB interferometer will become:

$$\begin{aligned} |\Psi^{R,m}\rangle &= |\Psi_{ref}^{R,m}\rangle + |\Psi_{QD}^{R,m}\rangle \\ &= \sum_{n \in R} (t_{ref} + t_{m,m}) e^{-ikn} |n, m\rangle + \sum_{n \in R, m' \neq m} t_{m',m} e^{-ikn} |n, m'\rangle. \end{aligned} \quad (\text{A4})$$

For the discussed situation, when the incoming channel in the left lead is m , the transmittance of the interferometer is noted by T_m and is defined as:

$$T_m = |\Psi^{R,m}|^2 = |t_{ref} + t_{m,m}|^2 + \sum_{m' \neq m} |t_{m',m}|^2. \quad (\text{A5})$$

Now we consider an incoherent lead for which the incident electron may come through each of the channels m with equal probability $1/M$. The total transmittance becomes:

$$\begin{aligned} T_{int} &= \frac{1}{M} \sum_m T_m = \frac{1}{M} \sum_{m, m'} [|t_{m, m'}|^2 + \delta_{m, m'} |t_{ref}|^2 \\ &\quad + 2\delta_{m, m'} |t_{m, m'}| |t_{ref}| \cos(\phi_{m, m'} - \phi_{ref})]. \end{aligned} \quad (\text{A6})$$

or, equivalently,

$$T_{int} = T_{dot} + |t_{ref}|^2 + \frac{2}{M} |t_{ref}| \sum_m |t_{m, m}| \cos(\phi_{m, m} - \Phi), \quad (\text{A7})$$

where $T_{dot} = 1/M \sum_{m, m'} |t_{m, m'}|^2$.

The last term in the interferometer transmittance formula accounts for the quantum interference and depends only on the diagonal dot tunneling processes $t_{m, m}$ that do not change the transport channel. The off-diagonal tunneling amplitudes $t_{m, m'}$ with $m \neq m'$ add up in module in Eq.A7 and their phases do not influence the total transmittance (nor can they be measured).

Appendix B: Multi-channel transport through a quantum dot

This Appendix aims to give an example (for the completeness of the paper) of how the tunneling amplitudes through a quantum dot can be calculated in terms of the dot Hamiltonian. See for instance [27, 28] for a similar demonstration using the Green functions approach. The method presented here calculates the scattering solution for the system wave function. Although it is a rather general method (for the case when one electron is scattered by a region with interaction and internal degrees of freedom), it is practical only for few-body problems. For many-body problems, the task of calculating the system wave function is not realistic, and one needs different approaches.

In this section, we use the same notation as in Appendix A and consider that the incident electron comes from the left lead through the channel m . The wave functions for the electron in the left and the right leads were already given in Eqs.A1,A3 and the wave function for the electron in the dot is:

$$|\Psi^{D,m}\rangle = \sum_{n_D \in D_{dot}, m'} c_{m',m}(n_D) |n_D, m'\rangle. \quad (B1)$$

n_D denotes a site in the quantum dot. The coefficients r , t (from Eqs. A1,A3) and c (from Eq. B1) are parametrically dependent of the incoming channel m , and will be determined from the Schrodinger equation:

$$\begin{bmatrix} H_D & H_{DL} & H_{DR} \\ H_{LD} & H_L & 0 \\ H_{RD} & 0 & H_R \end{bmatrix} \begin{bmatrix} |\Psi^D\rangle \\ |\Psi^L\rangle \\ |\Psi^R\rangle \end{bmatrix} = E \begin{bmatrix} |\Psi^D\rangle \\ |\Psi^L\rangle \\ |\Psi^R\rangle \end{bmatrix}. \quad (B2)$$

The leads Hamiltonian correspond to the discrete chain with the hopping between nearest neighbors taken equal with the energy unit:

$$H_{L(R)} = \sum_{n \in L(R), m'} (|n, m'\rangle \langle n+1, m'| + h.c). \quad (B3)$$

The coupling Hamiltonians are assumed not to change the channel, and account for the hopping of the electron between the dot site labeled $n_D = 0_{L(R)}$ and the site of the left (right) lead that is nearest to the dot and is labeled 1 (see Fig.2) (like in Eqs.A1-3 the lead site index does not need to carry the L or R - subindex, there is no danger of confusion):

$$\begin{aligned} H_{D,L(R)} &= \tau_{D,L(R)} \sum_{m'} |0_{L(R)}, m'\rangle \langle 1, m'|, \\ H_{L(R),D} &= \tau_{D,L(R)}^* \sum_{m'} |1, m'\rangle \langle 0_{L(R)}, m'|. \end{aligned} \quad (B4)$$

In the following, the coupling coefficients will be taken real and equal each other $\tau_{DL} = \tau_{DR} = \tau$.

From the solution in the lead, it is straightforward that the eigenenergy is $E = 2 \cos(k)$ (this is the dispersion solution for a discrete lead).

In order to calculate the system wave function, we need to first write explicitly the set of three equation from Eq.B2. The steps are outlined below:

1. One of the equations reads: $H_{LD}\Psi^D + H_L\Psi^L = E\Psi^L$. We use the explicit expression of wave function Ψ^L (Eq.A1) and write this equation for the site 1 of the left lead:

$$\begin{aligned} (e^{2ik}|1, m\rangle + \sum_{m'} r_{m',m} e^{-2ik}|1, m'\rangle) + \tau \sum_{m'} c_{m',m}(0_L)|1, m\rangle = \\ E(e^{ik}|1, m\rangle + \sum_{m'} r_{m',m} e^{-ik}|1, m'\rangle). \end{aligned} \quad (B5)$$

Using Eq.A3 for the right lead we have:

$$\sum_{m'} t_{m',m} e^{-2ik}|1, m'\rangle + \tau \sum_{m'} c_{m',m}(0_R)|1, m'\rangle = E \sum_{m'} t_{m',m} e^{-ik}|1, m'\rangle. \quad (B6)$$

One multiplies with $\langle 1, m'|$ on the left of Eqs. B5 and B6, and we have a relation between the dot wave function coefficients $c_{m',m}$ and the lead wave function coefficients, $r_{m'/m}$ and $t_{m'/m}$:

$$\begin{aligned} t_{m',m} &= \tau c_{m',m}(0_R), \\ r_{m',m} &= \tau c_{m',m}(0_L) - \delta_{m,m'}. \end{aligned} \quad (\text{B7})$$

2. The equation for the dot function reads: $H_D \Psi^D + \tau_{LD} \Psi_1^L + \tau_{RD} \Psi_1^R = E \Psi^D$. We introduce the explicit form of Ψ^L and Ψ^R from Eq.A1,A3 and we have:

$$H_D |\Psi_m^D\rangle + \tau (e^{ik} |0_L, m\rangle + \sum_{m'} r_{m',m} e^{-ik} |0_L, m'\rangle) + \tau \sum_{m'} t_{m',m} e^{-ik} |0_R, m'\rangle = E |\Psi_m^D\rangle. \quad (\text{B8})$$

Using the relation between the coefficients of the lead wave functions and dot wave function from Eqs.B7 one obtains (after some straightforward algebra) an equation for the coefficients $c_{m',m}$, which can be written in the compact form:

$$(E - H_{eff}^D) |\Psi_m^D\rangle = 2i\tau (\text{sink}) |0_L, m\rangle, \quad (\text{B9})$$

with

$$H_{eff}^D = H^D + \tau^2 e^{-ik} \sum_{m', \alpha=L,R} |0_\alpha, m'\rangle \langle 0_\alpha, m'| \quad (\text{B10})$$

3. Finally, the quantity of interest, the channel-dependent transmission coefficient, is:

$$t_{m',m} = 2i\tau^2 \sin(k) \langle 0_R, m' | \frac{1}{E - H_{eff}^D} |0_L, m\rangle. \quad (\text{B11})$$

- [1] A. Yacoby, M. Heiblum, D. Mahalu, H. Shtrikman, Phys. Rev. Lett. **74**, 4047 (1995).
- [2] R. Schuster, E. Buks, M. Heiblum, D. Mahalu, V. Umansky, H. Shtrikman, Nature **385**, 417 (1997).
- [3] D.C. Langreth, Phys.Rev. **150**, 516 (1966).
- [4] G. Hackenbroich, Phys. Rep. **343**, 463 (2001).
- [5] A. Aharony, O.E-Wohlman, Y. Imry, Physica E **29**, 283 (2005).
- [6] A. Aharony, O.Entin-Wohlman, B.I. Halperin, and Y.Imry, Phys.Rev.B **66**, 115311 (2002).
- [7] H.A. Weidenmuller, Phys. Rev.B **65**, 245322 (2002).
- [8] A. Levy Yeyati and M. Büttiker, Phys.Rev.B **62**, 7307 (2000).
- [9] Y. Oreg, New J. Phys. **9**, 122 (2007).
- [10] V. Kashcheyevs, A. Schiller, A. Aharony, and O. Entin-Wohlman, Phys. Rev.B **75**, 115313 (2007).
- [11] M. Avinun-Kalish, M. Heiblum, O. Zarchin, D. Mahalu, and V. Umanski, Nature **436**, 529 (2005).
- [12] M. Zaffalon, A. Bid, M. Heiblum, D. Mahalu, and V. Umansky, Phys.Rev.Lett **100**, 226601 (2008).
- [13] L.O. Baksmaty, C. Yannouleas, and U. Landman, Phys.Rev.Lett. **101**, 136803 (2008).
- [14] C. Karrasch, T. Hecht, A.Weichselbaum, J.von Delft, Y. Oreg, New J. Phys. **9**, 123 (2007).
- [15] A. Bertoni and G. Goldoni, Phys.Rev.B **75**, 235318 (2007).
- [16] S.A. Gurvitz, Phys.Rev.B **77**, 201302(R) (2008).
- [17] M.C. Goorden and M. Buttiker, Phys.Rev.Lett **99**, 146801 (2007).
- [18] A. Nishino, T. Imamura, N. Hatano, Phys.Rev.Lett **102**, 146803 (2009).
- [19] A. O. Govorov, Phys. Rev. B **70**, 035321 (2004).
- [20] G. Murthy, Phys. Rev. Lett. **94**, 126803 (2005).
- [21] R. K. Kaul, G. Zarand, S. Chandrasekharan, D. Ullmo, H. U. Baranger, Phys. Rev. Lett. **96**, 176802 (2006).
- [22] N.T.T. Nguyen and F.M. Peeters, Phys. Rev.B **76**, 045315 (2007).
- [23] J. Fernandez-Rossier, R. Aguado, Phys. Rev. Lett. **98**, 106805 (2007).
- [24] P.A. Mello, Y. Imry and B. Shapiro, Phys. Rev. B **61**, 16570 (2000).
- [25] S.K. Joshi, D. Sahoo, A.M. Jayannavar, Phys.Rev.B **64**, 075320 (2001).
- [26] S.S. Gylfadottir, M. Niță, V. Gudmundsson, A. Manolescu, Physica E **27**, 278 (2005)'
- [27] S. Datta, Electronic Transport in Mesoscopic Systems, Cambridge University Press (1995). See for instance Eq. 3.4.3.
- [28] P. Gartner and A. Aldea, Z. Phys. B **99**, 367 (1996).
- [29] J. König and Y. Gefen, Phys. Rev. Lett. **86**, 3855 (2001).
- [30] A. Aldea, M. Ţolea, J. Zittartz, Physica E **28**, 191 (2005).
- [31] T. Rejec, A. Ramsak, J.H. Jefferson, Phys.Rev.B **62**, 12985 (2000).